Letters

Current Oscillation Phenomenon of MMC Based on IGCT and Fast Recovery Diode With High Surge Current Capability for HVDC Application

Wenpeng Zhou, *Student Member, IEEE*, Biao Zhao, *Senior Member, IEEE*, Yantao Lou, Xiaoping Sun, Qi Liu, Ruihang Bai, *Student Member, IEEE*, Jiapeng Liu, *Student Member, IEEE*, Zhengyu Chen, Zhanqing Yu, *Member, IEEE*, and Rong Zeng, *Senior Member, IEEE*

***Abstract*—Integrated gate commutated thyristor (IGCT) has low loss, low cost, and high reliability in the application of modular multilevel converter (MMC). However, due to the special turn-OFF process of IGCT, the commutation transient is very different for IGCT in MMC. This letter reveals a current oscillation phenomenon of MMC based on IGCT and fast recovery diode (FRD). Especially, this oscillation effect becomes apparent when the FRD with high surge current capability is employed in MMC because of high junction capacitance and high stray inductance, which will threaten the safe operation of the system. This letter analyzes the current oscillation mechanism and gives the current oscillation modeling. In addition, through detailed tests under various stray inductances, the specific stray inductance range that can cause large current oscillation is obtained and an optimized inductance parameter of IGCT-MMC is proposed. The experiments show that the safe operation area of IGCT in MMC can be guaranteed maximally with the optimized parameter.**

***Index Terms*—Current oscillation, dc grid, high-voltage dc, integrated gate commutated thyristor (IGCT), modular multilevel converter (MMC).**

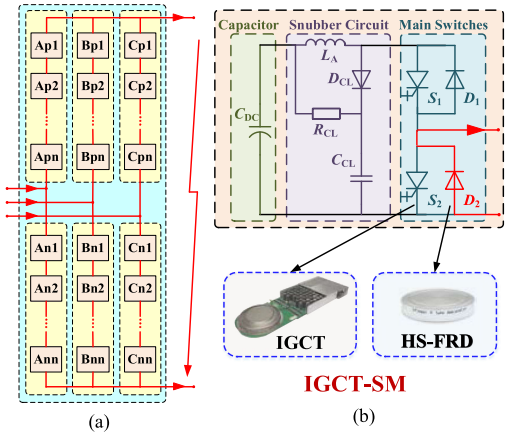

Fig. 1. Illustration of the dc pole-to-pole short circuit fault in IGCT-MMC system. (a) Paths of short current under the dc pole-to-pole short circuit fault. (b) IGCT-based MMC submodule (IGCT-SM) using HS-FRD to handle the short current under the dc pole-to-pole short circuit fault.

I. Introduction

RECENT years, integrated gate commutated thyristor (IGCT) has attracted much attention in the application of modular multilevel converter (MMC) [1], [2]. Compared with IGBT, IGCT has lower conduction voltage drop and manufacturing cost. In addition, the reliability of IGCT is also higher than that of IGBT and the long-term failure rate does not exceed 100 Fits [3], [4]. In MMC based on IGCT (IGCT-MMC), due to the positive feedback effects during the turn-ON process of IGCT, the commutating di/dt between IGCT and the freewheeling diode cannot be controlled by IGCT. As a result, fast recovery diode (FRD) with high di/dt capability is needed as well as a certain anode inductance [5].

The dc pole-to-pole short circuit fault is usually considered as the most severe in the MMC-based HVdc system, especially for half-bridge-based MMC. When the dc pole-to-pole short circuit fault happens, the ac circuit breaker will cutoff the fault current with about 100 ms time delay for half-bridge MMC [6]. Before the fault current is cutoff, all active devices are blocked and the lower diode will suffer the large fault current, as shown in Fig. 1. For the practical ±500 kV / 3000 MW MMC based HVdc systems in China [7], the lower diode needs to withstand a continuous five surge current up to 32 kA [6]. To bear the short circuit current, the FRD with high surge current capability (HS-FRD) is needed.

Different from IGBT as a type of transistor driven by voltage, IGCT is a type of thyristor driven by current, so the turn-OFF

Manuscript received October 11, 2020; revised November 3, 2020; accepted November 16, 2020. Date of publication November 27, 2020; date of current version February 5, 2021. This work was supported in part by the Key Projects of the National Natural Science Foundation of China (51837006) and in part by Integration Projects of National Natural Science Foundation of China-State Grid Joint Fund for Smart Grid (U1966602). *(Corresponding authors: Biao Zhao; Rong Zeng.)*

Wenpeng Zhou, Biao Zhao, Ruihang Bai, Jiapeng Liu, Zhengyu Chen, Zhanqing Yu, and Rong Zeng are with the Department of Electrical Engineering, Tsinghua University, Beijing 100084, China (e-mail: 18511829845@163.com; zhaobiao112904829@126.com; bairuihang@qq.com; 18811362403@163.com; chenzhengyu@mail.tsinghua.edu.cn; yzq@tsinghua.edu.cn; zengrong@tsinghua.edu.cn).

Yantao Lou, Xiaoping Sun, and Qi Liu are with the Department of HVDC Technology, Xian XD Power Systems Co., Ltd, Xi'an 710065, China (e-mail: louyt@xdps.com.cn; 289817457@qq.com; qliucn@live.cn).

Color versions of one or more of the figures in this article are available online at https://doi.org/10.1109/TPEL.2020.3041005.

Digital Object Identifier 10.1109/TPEL.2020.3041005

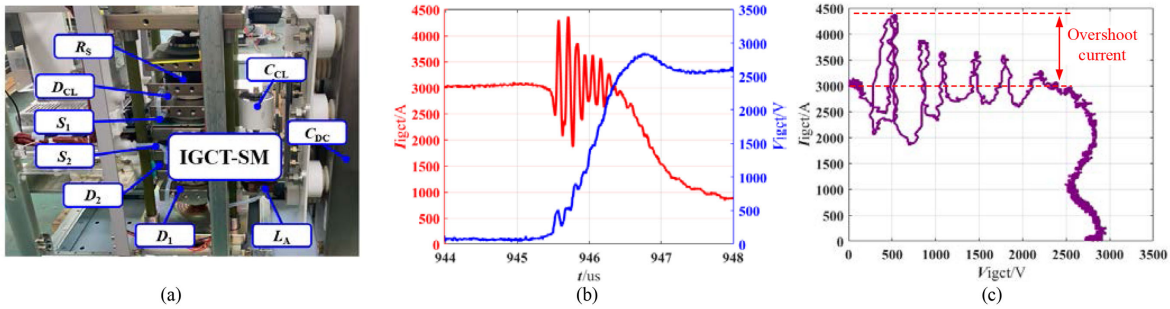

Fig. 2 (a) Photograph of a practical IGCT-SM. (b) Test results of IGCT's turn-OFF current and voltage with severe current oscillation. (c) I–V curve of IGCT's turn-OFF current and voltage showing the overshoot current.

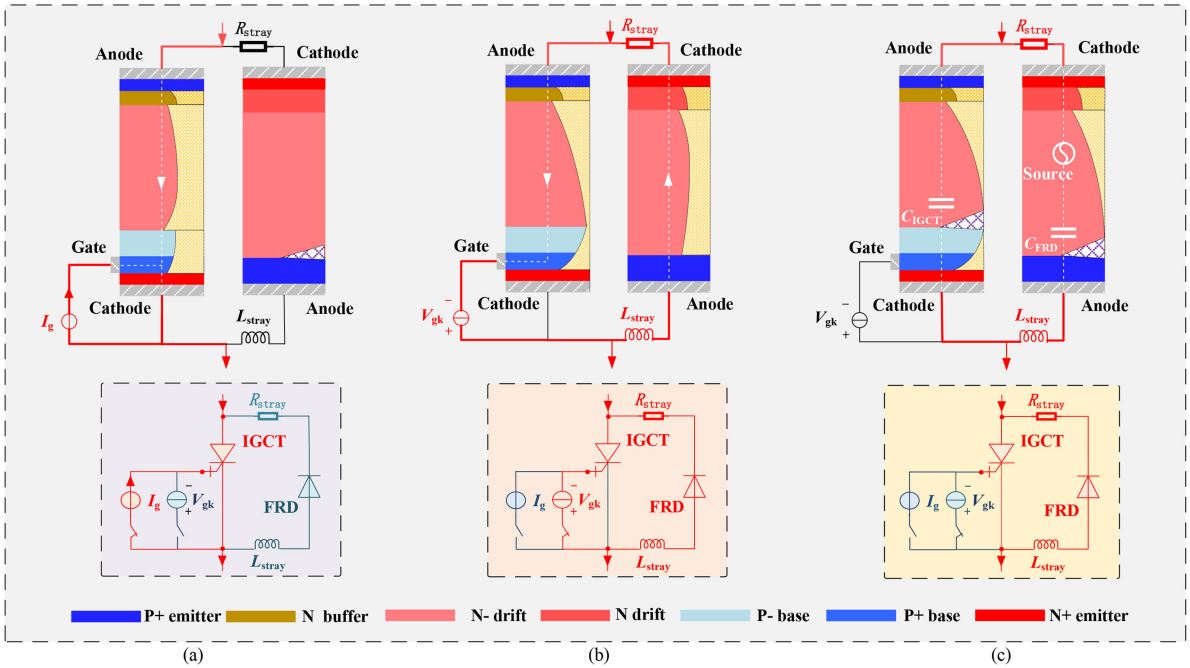

Fig. 3. Illustration of the current oscillation process between IGCT and FRD. (a) IGCT's conducting and FRD's blocking period. (b) IGCT's commutating and FRD's conducting period. (c) IGCT's anode building and current oscillating period.

commutation transient process of IGCT in MMC will be different, which brings special design considerations for IGCT's protection in IGCT-MMC. Though self-protection strategy with integrated PCB Rogowski coil in the gate driver is proposed as well as the protection system of IGCT-based converters [8]–[10], there are no analysis or experiments to handle this kind of issues for IGCT-MMC in literatures.

This letter reveals a current oscillation phenomenon of MMC based on IGCT and HS-FRD, and detailed analysis, design, and experiments are proposed.

II. Current Oscillation Phenomenon of IGCT-MMC With HS-FRD in Practice

Based on the practical ±500 kV / 3000 MW HVdc application based on MMC in China, a practical IGCT-SM is built, as shown in Fig. 2(a). The dc-link voltage is 2.2 kV and the rated-arm rms current is about 1700 A. In order to bear the dc pole-to-pole short circuit fault in HVdc system, HS-FRD is employed. Compared with general FRD for IGCT application, the surge current of HS-FRD is increased to double value, about 10 ms 70 kA, and the chip-size is also increased from 58 to 103.8 cm^2. In addition, in order to ensure enough current capability, HS-FRD should be pressed with higher pressure, which cannot withstand by IGCT, so a separate press structure is designed for HS-FRD in IGCT-SM.

In fact, because the arm current is sinusoidal, the peak value of arm current will reach about 3000 A when the rated-arm rms current is 1700 A. Fig. 2(b) gives a practical test waveform of IGCT-SM during the turn-OFF process when the turn-OFF current equals the peak current 3000 A. It can be seen that severe current oscillation occurs between lower IGCT and HS-FRD. The turn-OFF peak current of IGCT with the oscillation phenomenon achieves almost 4.5 kA and the overshoot current is nearly 1.5 kA.

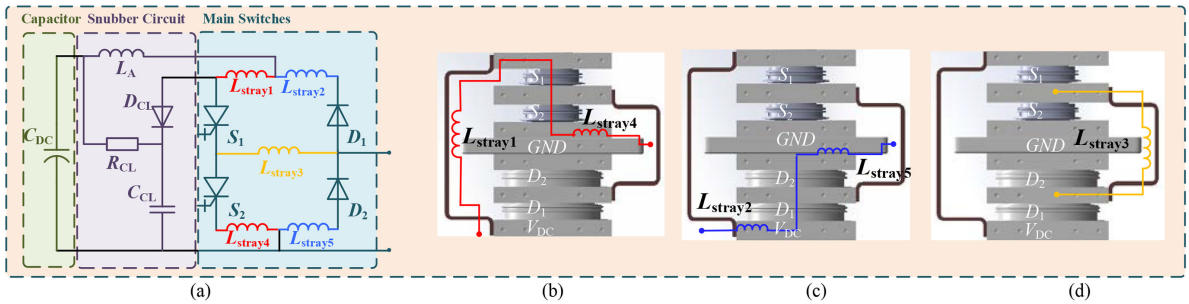

Fig. 4. (a) Equivalent circuit of IGCT-SM including stray inductances. (b) Positions of L_{stray1} and L_{stray4}. (c) Positions of L_{stray2} and L_{stray5}. (d) Position of L_{stray3}.

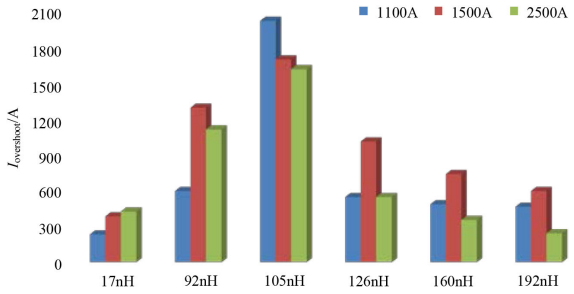

Fig. 5. Comparison of the overshoot currents in the oscillation between S2 and HS-FRD under different stray inductance and current conditions.

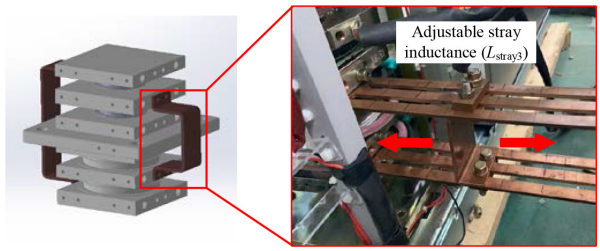

Fig. 6. Structure with an adjustable stray inductance.

In fact, different from IGBT, the maximum controllable current is a weakness for IGCT, so it is especially important to limit the peak current for IGCT application in practice. As for the IGCT-SM in Fig. 2(a), the maximum controllable current is 5 kA. If considering the current rising in the protection delay time of the controlling system in IGCT-SM, the turn-OFF current will exceed 3 kA. And, the turn-OFF peak current will exceed the maximum controllable current easily when the severe oscillation phenomenon still exists. Therefore, the current oscillation phenomenon of IGCT-MMC will threaten the safe operation of the system.

III. Current Oscillation Mechanism and Modeling of IGCT-MMC With HS-FRD in Practice

A. Current Oscillation Mechanism Analysis

Different from IGBT as a type of transistor driven by voltage, IGCT is a type of thyristor driven by current, so the turn-OFF process of IGCT-SM is very different.

Before IGCT turns OFF, all doping areas are full of lots of carriers to support the forward current and HS-FRD keeps reverse biased at this time, shown in Fig. 3(a).

When IGCT begins to turn OFF, the gate drive will apply a negative voltage (about 20 V) between the gate and cathode of IGCT and the cathode current is forced to commutate to the gate. During this period, the P-base region and N-drift region between the gate and anode are still filled with plenty of carriers, which has low voltage drops. Therefore, the voltage between anode and cathode is almost the same as the voltage between gate and cathode, which is about −20 V. The −20 V voltage is then applied on the anti-paralleled HS-FRD, which causes HS-FRD to be forward biased and establish a certain forward current during this period, shown in Fig. 3(b).

After IGCT completes the commutation process, it starts to build the blocking voltage rapidly. When HS-FRD gets reverse biased, it goes into the reverse recovery period. During this process, the depletion areas in IGCT and HS-FRD expand gradually, both showing certain capacitance effects, shown in Fig. 3(c).

In fact, as analyzed in Section II, because the HS-FRD is employed, there two separate press units in IGCT-SM, which increase the stray inductance between IGCT and HS-FRD. In addition, HS-FRD with a bigger chip size also increases the equivalent junction capacitance. Therefore, the current oscillation becomes apparent for IGCT-MMC with HS-FRD.

B. Current Oscillation Modeling

According to the analysis above, Fig. 3(c) shows an equivalent circuit of IGCT-SM during the current oscillation process. The equivalent junction capacitances of IGCT and FRD, together with the stray inductance and resistance form a resonance circuit that has the function of frequency selection. The excitation source caused by the reverse recovery process is a kind of nonideal transient waveform that can be decomposed into different frequency components. The total impedance and resonance frequency of the circuit are as follows. When the main frequency component is matched with the resonance frequency of the circuit, then severe oscillation of the main frequency component may happen

$$|Z| = \sqrt{{R_{\mathrm{stray}}}^2 + \left(\omega L_{\mathrm{stray}} - \frac{1}{\omega\left(C_{\mathrm{IGCT}}+C_{\mathrm{FRD}}\right)}\right)} \tag{1}$$

$$f_0 = \frac{\omega_0}{2\pi} = \frac{1}{2\pi\sqrt{L_{\mathrm{stray}}\left(C_{\mathrm{IGCT}}+C_{\mathrm{FRD}}\right)}}. \tag{2}$$

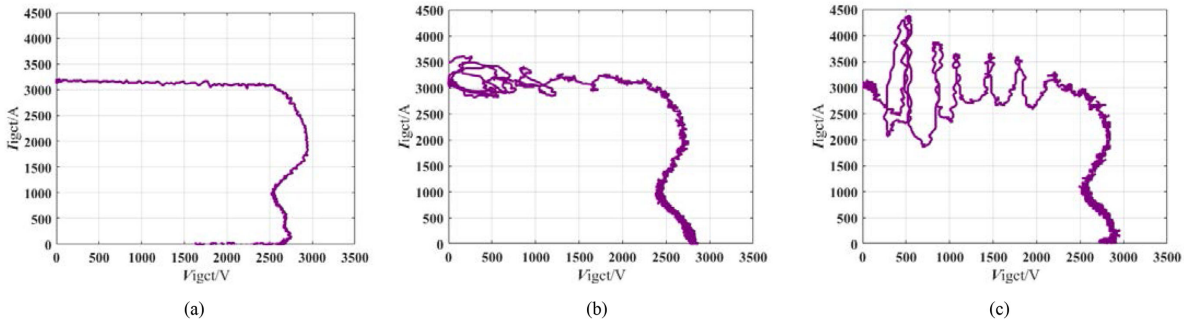

Fig. 7. Comparison of I–V curves of S2 at 3 kA. (a) Without anti-paralleled FRD. (b) Normal FRD is tested and the stray inductance is about 100 nH. (c) HS-FRD is tested and the stray inductance is about 100 nH.

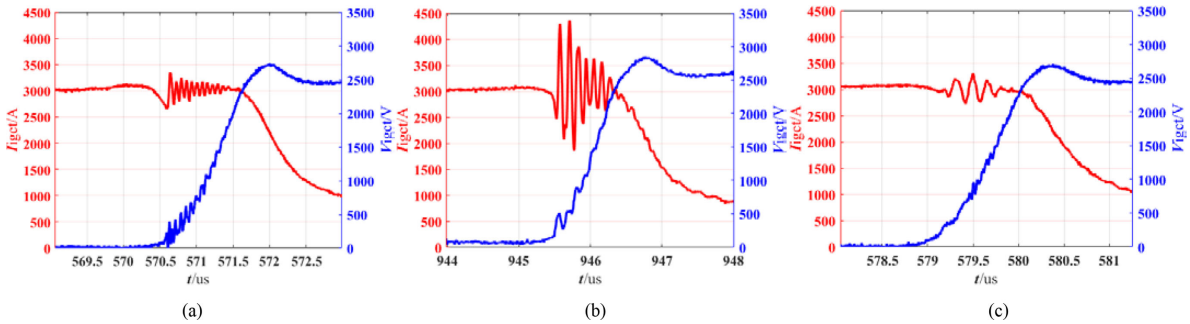

Fig. 8. Comparison of the oscillation waveforms of S2 at 3 kA under different stray inductances. (a) Stray inductance is below 20 nH. (b) Stray inductance is about 100 nH. (c) Stray inductance is over 150 nH.

From Fig. 3(c), the junction capacitances of the devices and the stray inductance will be the key to cause current oscillation. However, it is hard to estimate the capacitances and the excitation source accurately through numerical simulation with the usual model in the commercial software. But we can extract the stray inductance based on finite element analysis, then to get the oscillation rules through experiments.

In the designed structure of IGCT-SM, IGCTs and FRDs are pressed together following the sequence S_1, S_2, D_2, and D_1. The positions of stray inductances are shown in Fig. 4(b)–(d). Since S_1 and D_1 are at both ends of the structure, while S_2 and D_2 are in the middle position, the stray inductance between S_1 and D_1 is greater than that of S_2 and D_2. The extracted stray inductances using AnsysQ3d show that the total stray inductance between S_1 and D_1 is more than 200 nH, and the total stray inductance between S_2 and D_2 is about 100 nH.

Then the detailed tests in designed IGCT-SM are carried out between S_2 and D_2 under different stray inductances and current levels, as shown in Fig. 5. The changes of the stray inductance are realized in a special structure shown in Fig. 6. It is found clearly that the changing trends of the overshoot current following the stray inductances are almost the same under the same tested current levels. The changes of the overshoot currents following current levels under the same stray inductance may be caused by the nonlinear changes in the frequency components of the excitation sources.

The overshoot current achieves the peak value when the stray inductance is around 100 nH, with more than 1.5 kA at the tested current of 2.5 kA. This means that strong resonance is formed between S_2 and D_2 during the oscillation process at this stray inductance. And the overshoot current is suppressed greatly under stray inductance below 20 nH and over 150 nH, with less than 0.5 kA at the tested current of 2.5 kA.

IV. Experiment and Optimization of Current Oscillation Phenomenon for IGCT-MMC With HS-FRD

A. Current Oscillation of IGCT-SM With Different FRDs

To verify the previous theoretical analysis, turn-OFF tests of S_2 without FRD and with normal FRD are carried out and the I–V curves are compared in Fig. 7. It is found that there is no current oscillation when S_2 turns OFF without any antiparalleled FRD. The overshoot current is below 0.5 kA with normal FRD, while overshoot current is about 1.5 kA with HS-FRD. This means the main frequency component of the equivalent excitation source is not matched with the resonance frequency when normal FRD is tested with the stray inductance of about 100 nH.

B. Oscillation Optimization of IGCT-SM With HS-FRD

According to the analysis above, strong resonance is formed between S_2 and D_2 during the oscillation process at 100 nH stray inductance. And the overshoot current is suppressed greatly under stray inductance below 20 nH and over 150 nH. Final tests of 3 kA turn-OFF current under 2.2 kV dc-link voltage are compared to validate the proposed solutions. Figs. 8 and 9 show the oscillation waveforms and IV curves of IGCT-SM with HS-FRD after optimization respectively. It is found that the overshoot current of S_2 is decreased below 0.5 kA with 3 kA turn-OFF current under 2.2 kV dc-link voltage and the SOA of IGCT given in the datasheet can be guaranteed maximally.

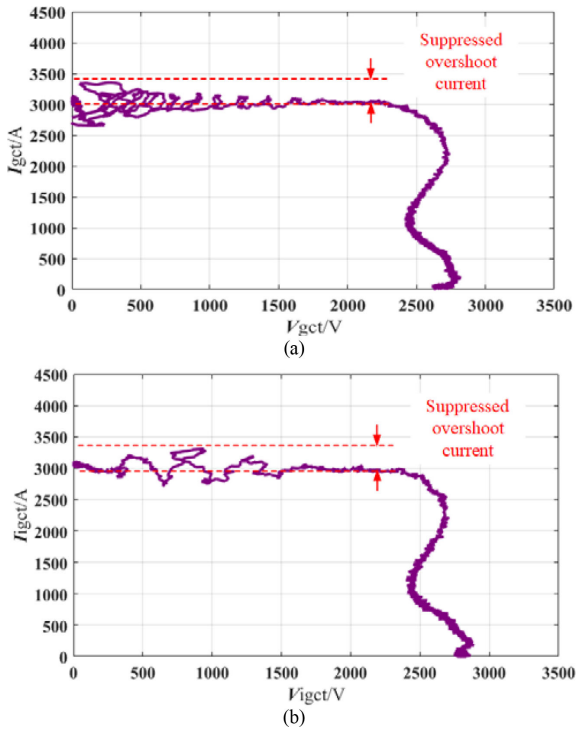

Fig. 9. Optimized IV curves with suppressed overshoot current during IGCT's turn-OFF process. (a) Stray inductance is below 20 nH. (b) Stray inductance is over 150 nH.

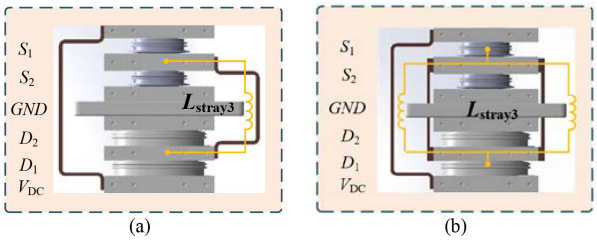

Fig. 10 Comparison of different structures of IGCT-SM with HS-FRD. (a) Before optimization. (b) After optimization.

From the oscillation waveforms shown in Fig. 8, it is easily found that different frequency components of the excitation source perform different characteristics when they get through the frequency selection circuit. According to the results, the component of about 8 MHz can be considered as the main frequency component in the equivalent excitation source. Meanwhile, the total equivalent junction capacitance C_{total} is about 4 nF through estimation by the following

$$C_{\text{total}} = C_{\text{IGCT}} + C_{\text{FRD}} = \frac{1}{{f_0}^2 4\pi^2 L_{\text{stray}}}. \tag{3}$$

To avoid the overvoltage risk, the stray inductance between S_2 and D_2 (HS-FRD) is optimized to be decreased. The current paths between S_2 and D_2 are shorten further and the stray inductance is below 20 nH, as shown in Fig. 10.

V. Conclusion

This letter reveals a current oscillation phenomenon of MMC based on IGCT and HS-FRD. From the letter, because of the special turn-OFF process of IGCT, the strong resonance is formed between IGCT and FRD, and this oscillation effect is especially apparent when the HS-FRD with high junction capacitance is employed. Because the maximum controllable current is a weakness for IGCT, the current oscillation will threaten the safe operation of the system. Through detailed tests under various stray inductances, the specific stray inductance range which can cause large current oscillation is obtained and an optimized inductance parameter of IGCT-SM is proposed. Comparison of experiments under the test current of 3 kA and 2.2 kV dc-link voltage shows that the overshoot current is decreased to 0.5 kA with the proposed optimized parameter of IGCT-MMC and the SOA of IGCT given in the datasheet can be guaranteed maximally.

References

[1] D. Weiss, M. Vasiladiotis, C. Banceanu, N. Drack, B. Odegard, and A. Grondona, "IGCT based modular multilevel converter for an AC-AC rail power supply," in *Proc. PCIM Eur. Int. Exhib. Conf. Power Electron., Intell. Motion, Renew. Energy Energy Manage.*, 2017, pp. 1–8.

[2] B. Zhao *et al.*, "A more prospective look at IGCT: Uncovering a promising choice for dc grids," *IEEE Ind. Electron. Mag.*, vol. 12, no. 3, pp. 6–18, Sep. 2018.

[3] P. Ladoux, N. Serbia, and E. I. Carroll, "On the potential of IGCTs in HVDC," *IEEE J. Emerg. Sel. Top. Power Electron.*, vol. 3, no. 3, pp. 780–793, Sep. 2015.

[4] M. Buschendorf, J. Weber, and S. Bernet, "Comparison of IGCT and IGBT for the use in the modular multilevel converter for HVDC applications," in *Proc. Int. Multi-Conf. Syst., Signals Devices*, 2012, pp. 1–6.

[5] R. Zeng *et al.*, "Integrated gate commutated thyristor-based modular multilevel converters: A promising solution for high-voltage dc applications," *IEEE Ind. Electron. Mag.*, vol. 13, no. 2, pp. 4–16, Jun. 2019.

[6] H. Chen, F. Wakeman, J. Pitman, and G. Li, "Design, analysis, and testing of PP-IGBT-based submodule stack for the MMC VSC HVDC with 3000 A DC bus current," *J. Eng.*, vol. 2019, no. 16, pp. 917–923, Mar. 2019.

[7] H. Pang and X. Wei, "Research on key technology and equipment for Zhangbei 500kV DC grid," in *Proc. Int. Power Electron. Conf.*, 2018, pp. 2343–2351.

[8] H. Zeng *et al.*, "An IGCT anode current detecting method based on Rogowski coil," in *Proc. IEEE Appl. Power Electron. Conf. Expo.*, 2017, pp. 1480–1483.

[9] H. Zeng *et al.*, "IGCT self-protection strategy for IGCT converters," in *Proc. 10th Int. Conf. Power Electron. ECCE Asia*, 2019, pp. 793–798.

[10] C. Wang *et al.*, "Investigation on the protection system of the large power converter with IGCT," in *Proc. 7th Int. Power Electron. Motion Control Conf.*, 2012, pp. 1603–1606.